



DESIGN AND TEST OF AN ADVANCED SYSTEM FOR ENERGY GENERATION

High-Performance Gas Turbine Engine and Permanent Magnet Generator with Foil Bearings,
Controlled by a Multi-Level Inverter

Dr. Daejong Kim
Associate Professor Mechanical and Aerospace Engineering
University of Texas at Arlington
Arlington, TX, United States

John O'Connor
President
Oztek Corporation
Merrimack, NH, United States

Friedhelm Schwenne
Principal Engineer
Elektromaschinen und Antriebe AG (e+a)
Möhlhlin, Switzerland

Mike Drumm
President & CEO
ExSell Motors
Concord, CA, United States

ABSTRACT

This paper presents the design of an advanced Power Generation System using a Gas Turbine Engine (GTE), oil free bearings, high-speed Permanent Magnet (PM) Generator and Multi-Level Pulse Width Modulated (PWM) Inverter. Torque is transmitted through a specially designed flexible coupling and foil bearings are used in both the PM generator and gas turbine engine. The systems covered by this paper consist of a 140KW, 64,000 RPM PM Generator that is connected via a flexible coupling to a Gas Turbine Engine with foil bearings, and a 160KW, 51K RPM PM Generator that is connected to Gas Turbine Engine that uses fluid film bearings; both systems are controlled by a Multi-Level Grid-Tie Inverter (MLI). The paper is focused principally on the design of the foil bearings for the 140KW PM Generator, the design of the Permanent Magnet Generator, and the development of the Multi-Level Inverter.

INTRODUCTION

Commercial designs of low voltage (<1000V & up to 2MW of power) energy generation systems based on gas turbine engines, have, until even fairly recently, consisted of a Gas Turbine Engine running on Journal/Fluid Film Bearings, connected through a gearbox with its associated oil lubrication system to a large, low-speed, 50/60 Hz generator, that is then controlled via a standard, low-frequency inverter. Disadvantages of these class of systems are normally large size, use of oil lubrication for both bearings and the gearbox, lower efficiency and significantly lower reliability due to the mechanical step-down in speed provided by the gearbox and cooling loop associated with the oil system, plus thermal losses in the standard motor/generator caused by using an induction machine. Low cost achieved by being able to take advantage of a machine wound stator in the low-speed generator is normally more than offset by the requirement of the bulky gearbox and supporting oil system.

A more advanced, compact and efficient system can be designed using oil free bearings, avoiding the gearbox entirely by employing a direct-drive, high-speed Permanent Magnet (PM) generator that matches the shaft speed of the GTE. The generator can be used initially as a motor to start the gas turbine engine, then switch automatically into generator mode when power begins to flow out; torque is transmitted through a high-speed, flexible coupling, and a Multi-Level PWM Grid-Tie Inverter (MLI) is used to interface to the AC line and also provide a clean current

signal with low Total Demand Distortion (TDD) to the generator without having to employ a sine filter to lower current ripple to an acceptable level. For simplicity, efficiency and low cost, foil bearings are used in both the GTE and PM generator. Foil bearings can be used successfully in most high-speed, “low voltage” applications up to approximately 2MW in power.

Challenges in the development of this advanced high-speed system include the specification, design, manufacture and integration of foil bearings into the GTE and PM generator; the design of the flexible coupling; the design of a reliable, robust and efficient high-speed PM generator able to sustain the required high circumferential speed; the design of a cooling system for the generator and inverter that includes both liquid cooling around the stator of the generator and Power Modules (IGBTs) in the inverter, and air cooling through the air gap in the PM generator and throughout the cabinet in the MLI. A comprehensive rotordynamic model and analysis is critical to the success of the project as is the development of test fixtures, tools and test strategies to provide both component, sub-system and system level testing in an effort to reduce project complexity and risk.

A project as described above was initiated in 2017 by a large manufacturer of classical Industrial Gas Turbine Engine Generators with gear box and low speed generator, with the expressed goal of significantly reducing the footprint, lowering the cost, and increasing the reliability of their existing line of Generators (nominally 160KW running at 51,000 RPM), then eventually expanding the line into higher power machines up through 2 MW (18,000 RPM). The initial project focused on the following efforts:

- Development of a prototype test bench consisting of a 100KW, 51,000 RPM system to prove direct-drive generator and foil bearing feasibility. This was designated as the ALPHA system and hardware resulting from this design is shown in Figure 1, where the ALPHA generator was connected to an induction motor with a flexible coupling for a rotordynamics spin test. The system was successfully tested to full speed; then the ALPHA system was connected directly to an existing GTE using a flexible coupling for additional rotordynamic evaluation. Based on the confidence built from the ALPHA hardware and these initial testing successes the project expanded into the efforts described below.
- The power of the ALPHA PM Generator was increased to 160KW, maintaining the 51,000 RPM rated speed; the gear box, standard low speed motor and relevant oil system was replaced with a 160KW/51,000 RPM PM generator and MLI inverter. This new generator sub-system was designated as GAMMA and hardware for this design is shown in Figure 2 (left). A GAMMA PM generator was connected to a legacy GTE with fluid film bearings and a two stage axial turbine with a flexible coupling (Figure 2, right). An initial spin test of the GAMMA PM generator at full speed is shown in Figure 3.
- Development of a new, higher speed GTE and associated generator system targeted at 140KW and running at 64,000 RPM. The new GTE design included foil bearings in place of the older fluid film bearings, a radial turbine in place of the previous two stage axial turbine, a new compressor with higher efficiency, a faster speed (64K RPM vs. 51K RPM), revised air & cooling flow, and a higher Pressure Ratio (4.5 vs. 3.5). The new GTE was designated the E100F. The new generator sub-system (designated as BETA) included a PM generator with foil bearings, a flexible coupling to transmit torque from the new GTE to the generator, and a Multi-Level Inverter to provide control and to interface the generator to the grid. Hardware for the Beta system is shown in Figure 4.

The goal was to use a common design of PM generator for both the 140KW and 160KW systems, with an identical frame size (same stator outside diameter (OD)) differing only in stator and rotor length to achieve the additional power required, and a single design of a Multi-Level Inverter to power both 140KW and 160KW systems.

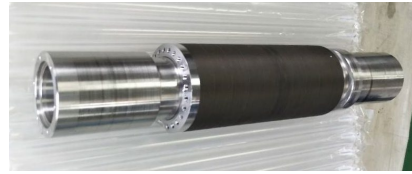
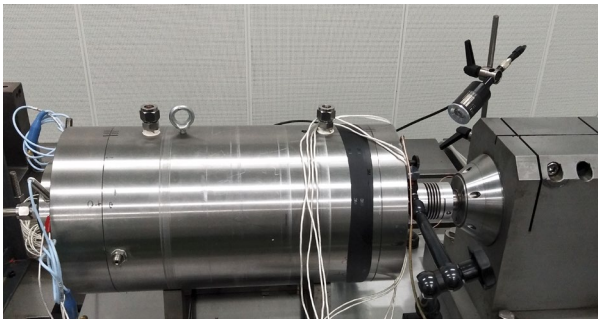


Figure 1: Alpha Hardware Connected to Induction Motor through Flexible Coupling (Left); Alpha Generator Shaft Assembly (Right)



Figure 2: Gamma Generator Hardware (Left) and Test Rig with Legacy GTE Using Fluid Film Bearing

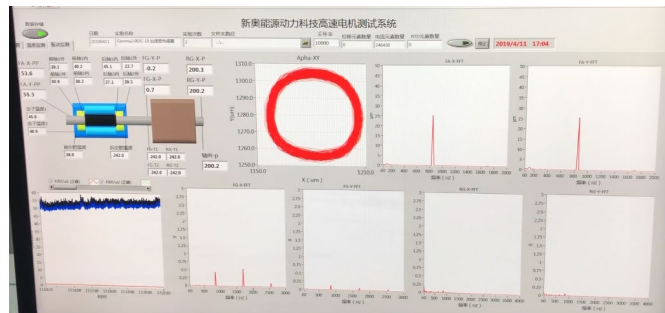


Figure 3: Screen Shot from GAMMA PM Motor Test at Full Speed (51,000 RPM)



Figure 4: Beta Hardware in Housing

CONCEPTUAL DESIGN

This paper will concentrate on the design and test of the BETA PM Generator and the Multi-Level Inverter but will reference other elements of the project in diagrams and descriptions. Shown below in Figure 5 is the entire Beta rotor-bearing-coupling conceptual design used for developing the rotordynamic model. The elements of the design consist of the:

- Generator Shaft
- Permanent Magnet Rotor with Carbon Fiber Retaining Sleeve
- Flexible Coupling
- E100F Compressor, Shaft and Turbine

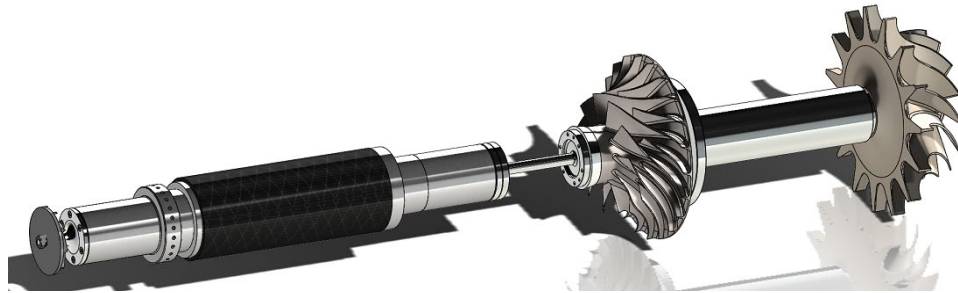


Figure 5: Entire Rotor Assembly of Beta PM Generator and E100F GTE with Flexible Coupling

The conceptual model and actual hardware for the Beta PM Generator is shown in Figure 6 (Left) and (Right). The electromagnetics consist of a tapered shaft inserted into a steel mandrel that holds the permanent magnets that are then covered with a carbon fiber overwrap. A laminated stator made of high-frequency steel encloses the rotor that is supported by 1.96 in. (50mm) foil bearings on both sides of the stator end-turns. The stator is shrunk into a steel cooling jacket with O-rings mounted on each end, then fitted into a housing that provides the outside enclosure for the cooling jacket. The 3-phase cables and the thermocouple wires exit the stator through the bearing housing on the left end and the flexible coupling is attached to the generator shaft and the E100F rotor string on the opposite side. Cooling air flows through the air gap between the rotor and stator to assist in rotor and shaft cooling and a water/glycol mixture is pumped through the cooling jacket to remove stator thermal losses.



Figure 6: 140KW Generator Test Rig: Solid Model (Left) & Actual Hardware (Right)

Figure 7 presents the 140KW Beta Generator with air flow passage to the compressor over the flexible coupling. The flow passage also serves as a mechanical structure connecting the generator and GTE. Due to the flow structure

enclosing the flexible coupling, a catching mechanism of the coupling is implemented inside the generator rotor to allow easy engage/disengage of the generator from the GTE.

The generator produces 140KW running at 64,000 RPM on foil bearings. Figure 7 shows a spin test rig platform that was designed for the entire turbo alternator considering compressor flow passages and using a dummy compressor impeller and an impulse turbine drive. The test rig platform can be used for spin test using just the impulse turbine as a main drive or a motor-assisted turbine drive during start up. Figure 8 shows a photo of stand-alone hardware used for spin testing the E100F GTE rotor, which is the enclosed portion in the red dashed box in Figure 7.

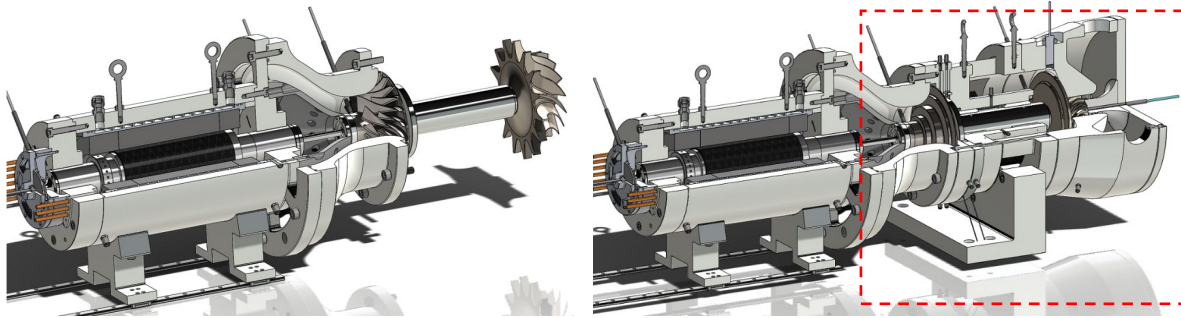


Figure 7: 140KW Generator with GTE Rotor with Air Flow Passage Around Compressor (Left); Spin Test Rig Platform Using Dummy Compressor and Impulse Turbine (Right)



Figure 8: Photo of Stand-Alone Spin Test Rig Platform for E100F GTE

ROTORDYNAMIC MODEL

Figure 9 shows a 3-D image of the entire Beta rotor and its associated discretized beam model. Figure 10 is the undamped critical speed map (UCS) of the Beta rotor with foil bearing stiffness overlapped. The diaphragm coupling stiffness was calculated separately and the diaphragm coupling was replaced by an equivalent beam shaft coupling with the same stiffness as the original diaphragm coupling. Rigid body modes are both below 20,000 RPM and the first bending mode is over 130,000 RPM.

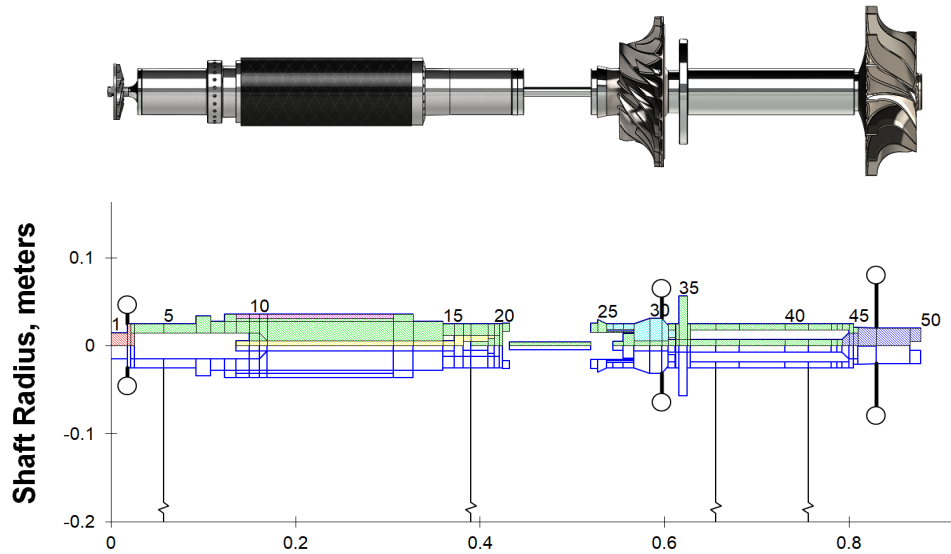


Figure 9: Beta Rotor Solid Model in 3-D (Top) and Discretized Beam Model (Bottom)

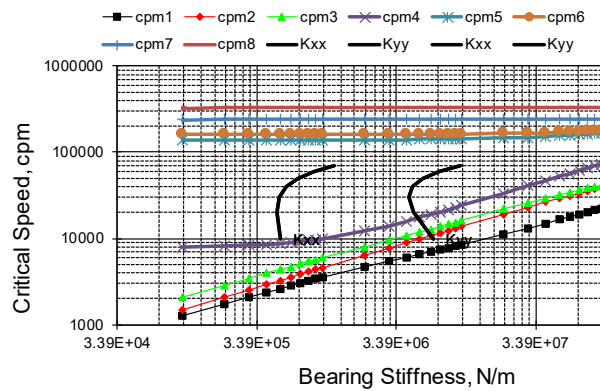


Figure 10: Undamped Critical Speed Map of Beta Rotor (UCS)

BEARING DESIGN FOR BETA SYSTEM

Figure 11 is a picture of the 1.96 in. (50mm) Beta foil bearing, and also shows the bearing installed in the Beta Generator. Figure 12 is a picture of a 4.33 in. (110mm) axial foil bearing with Teflon coating for the test rig in Figure 8, but bearings for the actual E100F GTE are designed with a high temperature coating 1,228°F (650°C) maximum.

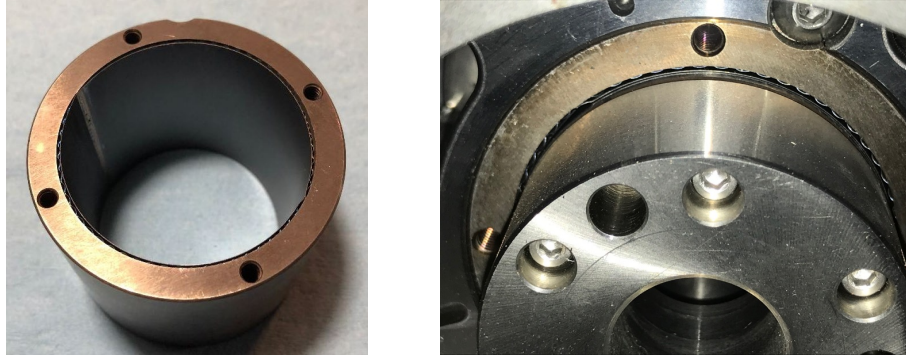


Figure 11: Picture of 1.96 in (50mm) Foil Bearing for Beta PM System (Left); Picture of Foil Bearing Installed in Beta System (Right)



Figure 12: Picture of 4.33 in. (110mm) Axial Foil Bearing for E100F GTE; Shown with Teflon Coating for Test Rig in Figure 8

Bearing stiffness and damping coefficients of the 1.96 in, (50mm) bearing for the Beta system were calculated using in-house code developed at the University of Texas at Arlington (UT-Arlington). In addition, modal impedances of the bearing can be found using Eq. (1) and (2) below. Real and imaginary parts of the following expression are modal stiffness and damping for forward whirling motion, respectively.

$$Z_f = \frac{k_{XX} + jd_{XX}\omega_s + k_{YY} + jd_{YY}\omega_s}{2} - \sqrt{\left(\frac{k_{XX} + jd_{XX}\omega_s - k_{YY} - jd_{YY}\omega_s}{2}\right)^2 - (k_{XY} + jd_{XY}\omega_s)(k_{YX} + jd_{YX}\omega_s)} \quad (1)$$

If the direct terms are equal ($k_{XX} = k_{YY}$, $d_{XX} = d_{YY}$) and there are no cross-coupled stiffness and damping in the bearing, then Equation (1) leads to:

$$Z_f = k_{YY} + jd_{YY}\omega_s \quad (2)$$

Therefore, the modal stiffness and damping are the effective stiffness and damping of the bearing along the forward rotor whirling orbit.

Figure 13 are stiffness and damping coefficients of the Beta bearing at 70,000 RPM as a function of excitation-frequency. Due to the design characteristics (strong anisotropy) of the bearing, stiffness along the gravitational loading direction (X-direction) is much larger than that along the Y-direction. The strong anisotropic feature of the bearing combined with small cross coupled stiffness results in a modal stiffness of around $8.2e4$ lb/ft ($1.2e6$ N/m) as shown in the modal impedance curve, Figure 14. It is also noteworthy that for the entire excitation frequency range, modal damping is positive, which means the bearing is stable for all external disturbances within the full frequency spectrum. Figure 15 presents synchronous bearing stiffness and damping coefficients as a function of speed. Table 1 shows the numerical values of stiffness and damping coefficients in Figure 15..

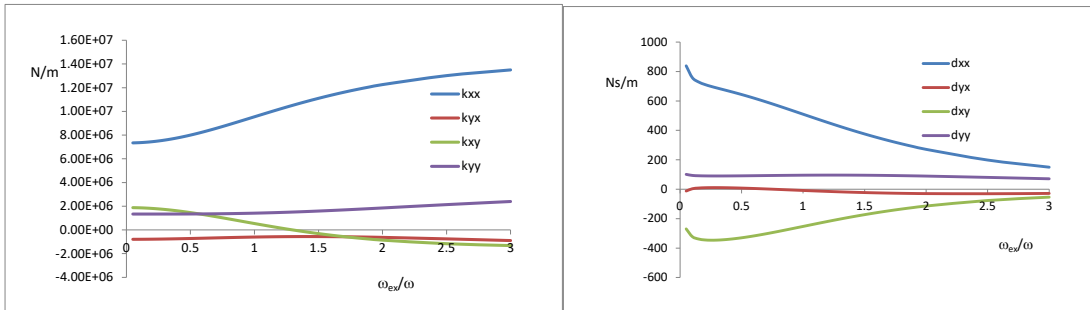


Figure 13: Stiffness (Left) and Damping (Right) Coefficients of Beta Bearing at 70,000 RPM
X: vertical direction Y: horizontal direction

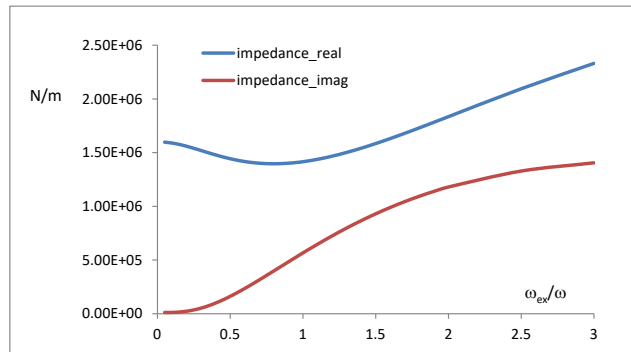


Figure 14: Modal Impedance Contour of Beta Bearing at 70,000 RPM

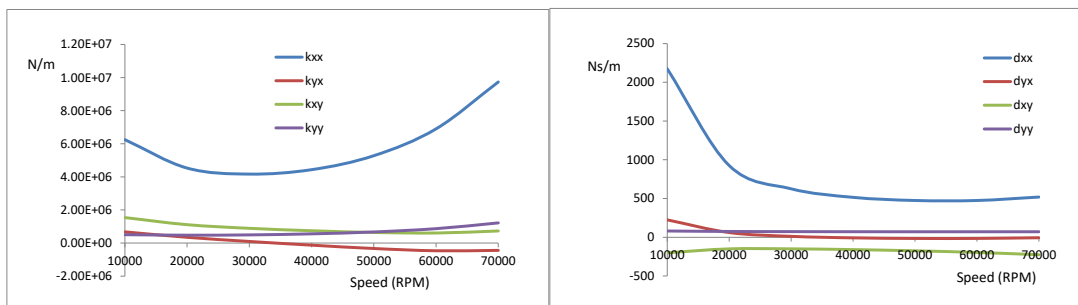


Figure 15: Synchronous Stiffness (Left) and Damping (Right) Coefficients of Beta Bearing as a Function of Speed;
X: vertical direction Y: horizontal direction

Table 1: Numerical Values of Stiffness and Damping Coefficients in Figure 15

Speed	kxx	kyx	kxy	kyy	dxx	dyx	dxy	dyy
10000	5.96E+06	727899	1.59E+06	561438	2163.66	255.346	-190.383	102.1
20000	4.25E+06	400048	1.18E+06	544255	934.654	91.4404	-141.351	95.6072
30000	3.83E+06	142963	949571	557082	616.379	29.2593	-144.898	92.7183
40000	3.97E+06	-102422	768357	607928	491.037	-1.71365	-158.329	90.5844
50000	4.59E+06	-339076	618229	713293	441.186	-15.1375	-175.794	89.3528
60000	5.84E+06	-537700	503603	899767	429.983	-17.0345	-196.473	89.2687
70000	8.03E+06	-623070	476309	1.22E+06	451.675	-10.615	-223.157	90.4843

Figure 16 is the damped natural frequency map of the Beta Bearing with 1X curve. All rigid body modes are below 20,000 RPM and there is a crossing of the 1X line with a backward bending mode at around 62,000 RPM.

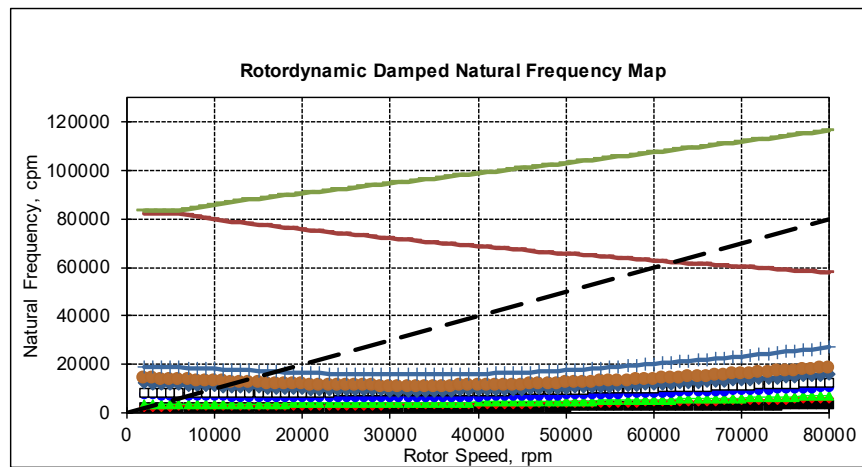


Figure 16: Damped Natural Frequency Map of Beta Bearing

IMBALANCE RESPONSE PREDICTED USING LINEAR BEARING COEFFICIENTS

This section presents the predicted imbalance response from commercial software using linear bearing coefficients of the foil bearings. Imbalance distributions used for prediction are shown in Figure 17.

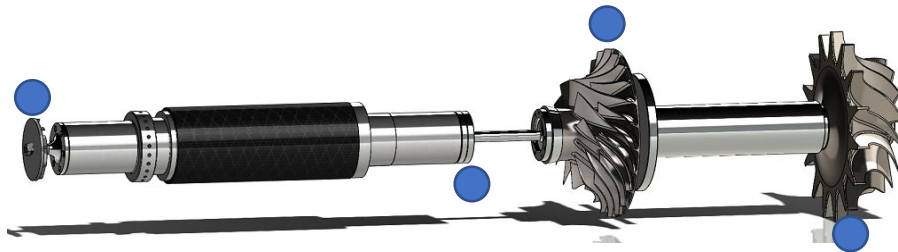


Figure 17: Imbalance Schemes Used in the Predictions; Out-of-Phase Imbalance of 2g-mm

Figure 18 and Figure 19 show the predicted bode plot of the out-of-phase imbalance response at the generator and GTE respectively, and Figure 20 and Figure 21 present predicted dynamic bearing reaction force due to an out-of-phase imbalance of 2g-mm. Bearing force is maximum at critical speeds and decreases as the rotor reaches a steady state operating speed of 80,000 RPM.

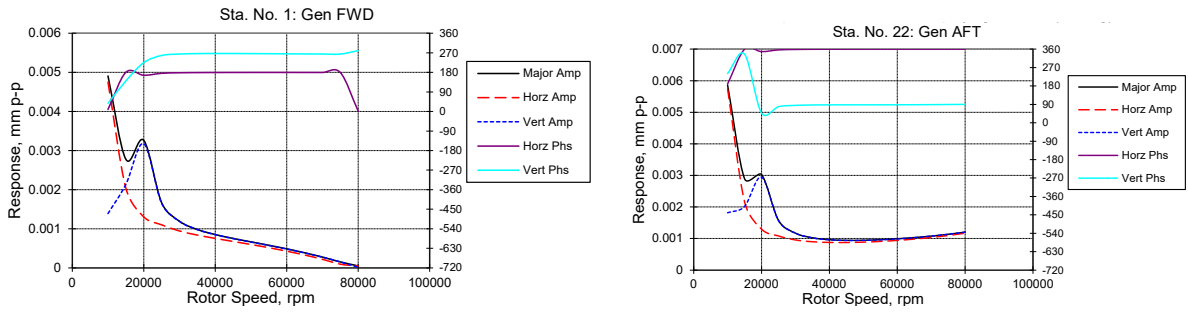


Figure 18: Predicted Out-of-Phase Imbalance Response at Beta Generator

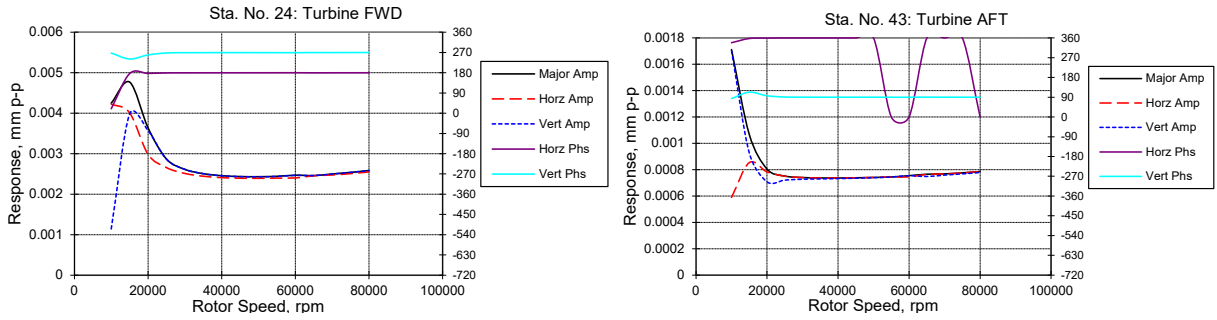


Figure 19: Predicted Out-of-Phase Imbalance Response at E100F GTE

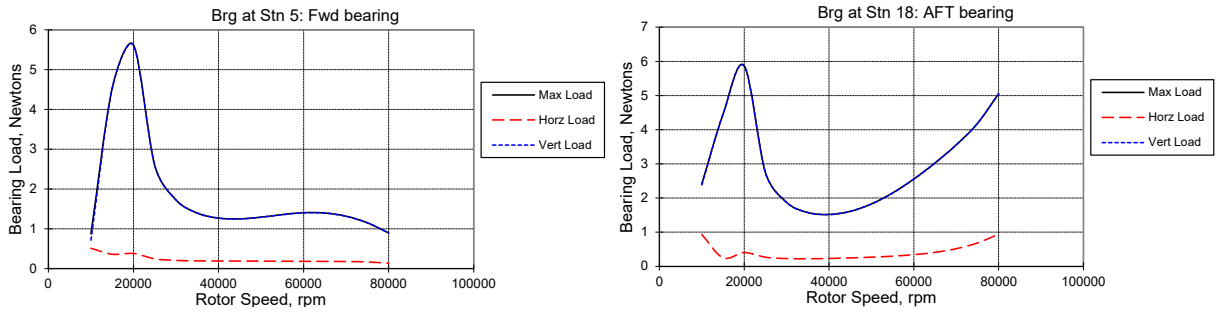


Figure 20: Predicted Bearing Dynamic Reaction Force at Beta Generator

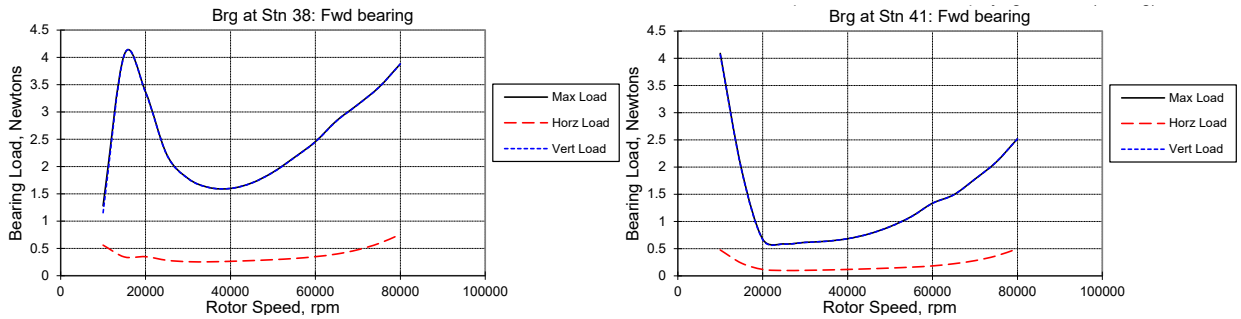


Figure 21: Predicted Bearing Dynamic Reaction Force at E100F GTE

3-D ROTORDYNAMIC ANALYSIS

This section presents 3-D non-linear rotordynamic analyses. The non-linear simulation solves rotor motion and Reynolds equations applied to each foil bearings at the same time, and it is more accurate in predicting any potential instabilities. Because the bending mode of each rotor is very high, the two rotors are modeled as rigid rotors and the coupling shaft is modeled as a beam element with the same stiffness as the diaphragm coupling. Detailed methods are presented in [Kim 2013]. Figure 22 presents the coordinate system and variables for the 3-D Rotordynamic Simulation of the Beta Generator and Turbine Shaft.

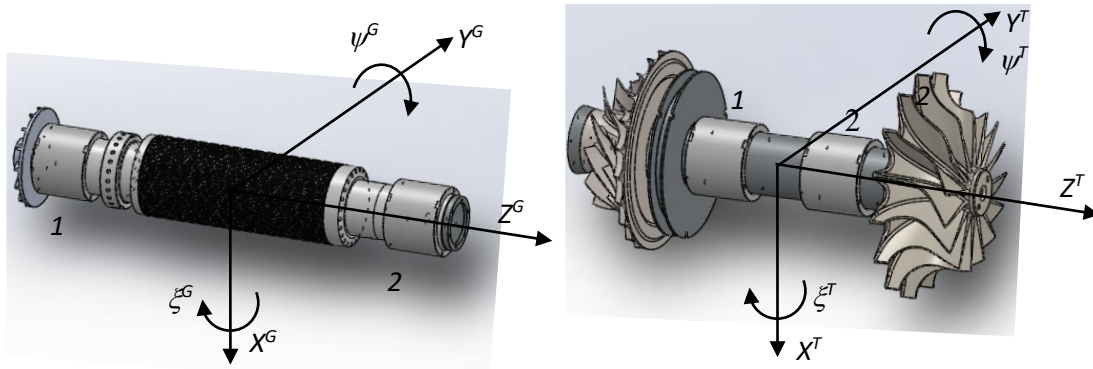


Figure 22: Coordinate System and Variables for 3-D Rotordynamic Simulation of Beta Generator and Turbine Shaft; 4-DOF model for Generator (Left) and GTE (Right)

Imbalances are applied as out-of-phase similar to Figure 17, and predicted responses are presented.

Figure 23 presents transient and steady state responses. The transient response is basically a drop simulation; initial (at $t=0$) rotor positions are at the center of the bearing and initial velocities of the rotor are also zero, which means the rotor spins at 70,000 RPM with the rotor at the centered position within the bearing and it is released under gravity at $t=0$. A close look of the transient responses shows typical 2nd order dynamics.

Figure 24 shows the bearing reaction forces. Total bearing forces are a summation of static loading (weight) and dynamic bearing forces. It is also noted that the horizontal reaction force is very small, almost invisible.

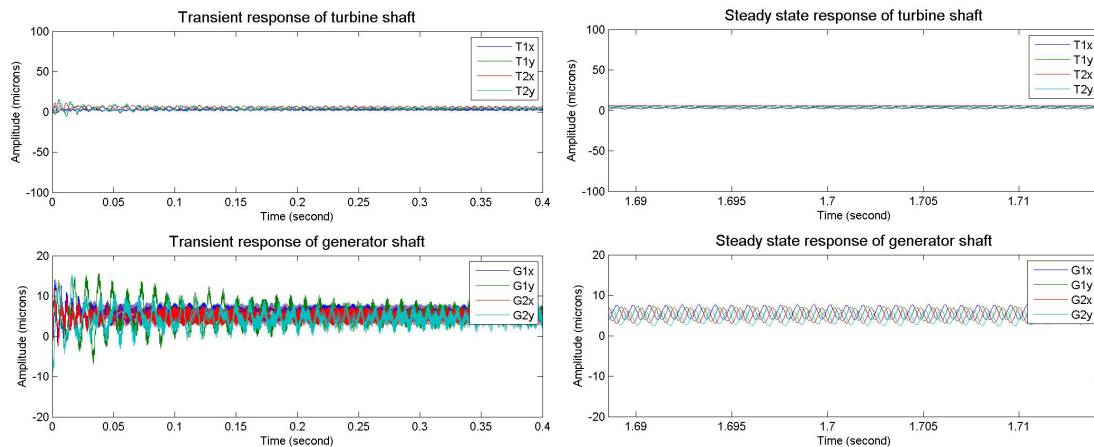


Figure 23: Transient (Left) and Steady State (Right) Responses for Beta Generator & Turbine Shaft

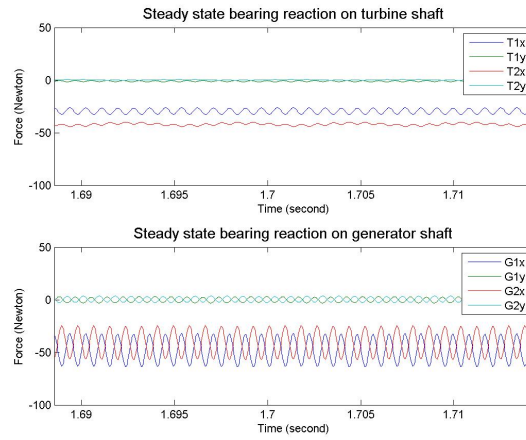


Figure 24: Bearing Reaction Forces for Beta Generator & Turbine Shaft

ELECTRO-MAGNETIC DESIGN – PM GENERATOR

The Beta generator has an S1 (continuous duty) power output of 140KW, at a rated speed of 64,000 RPM. The energy density and product complexity of high-power motors and generators tend to increase as a function of the combination of power and speed in a single package. As an illustration refer to Figure 25, which is a depiction of Relative Product Complexity using a graph of Power vs. Speed for a wide variety of motors and generators.

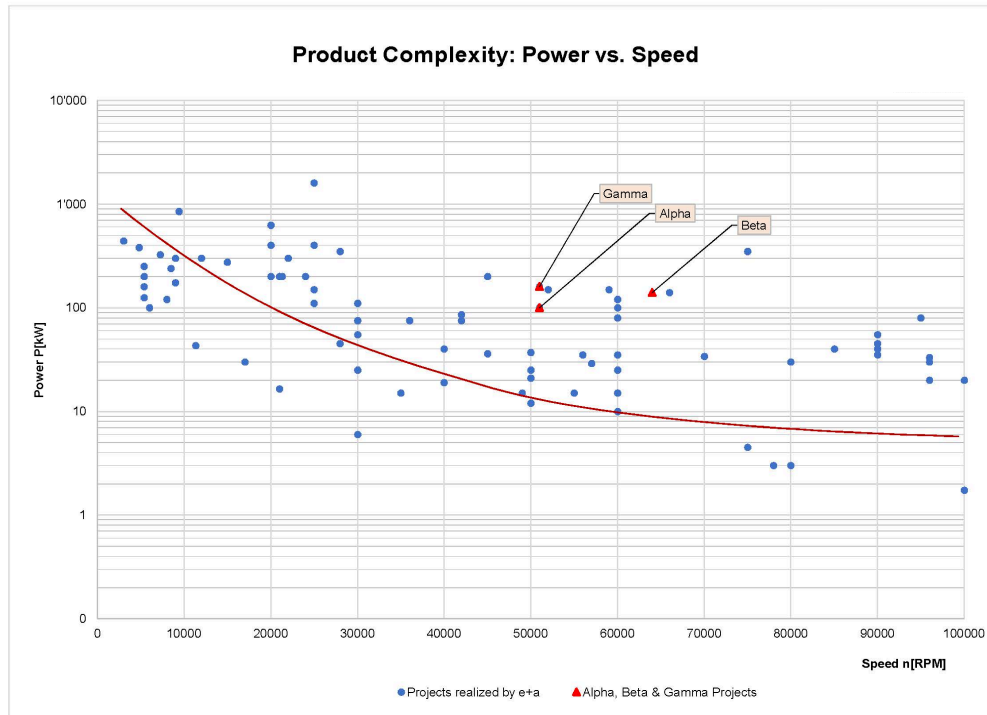


Figure 25 Relative Product Complexity

All motors and generators below the red line have a nominal design complexity and can be produced with little design risk. As the combination of power and speed gets larger the more capable and higher energy density designs move up and to the right, and the design complexity along with the power density continues to increase. The Beta motor/generator has the highest product complexity of the three products in this project, and a fairly high overall complexity compared to other realized projects.

The Beta Generator has a rotor with segmented Permanent Magnets attached to a steel mandrel, then covered with a carbon fiber overwrap. Special magnet shapes and arrangements are used in high-speed 2-pole rotors to reduce parasitic effects like additional rotor heating and torque ripples. The carbon fiber sleeve allows the Beta Generator to operate at a tip speed of 550.3 MPH (246 meters/second). Use of carbon fiber sleeves to wrap rotors and retain magnets in machines with high tip speeds is critical to achieve the reliability, full rated performance and safety in systems producing high centrifugal loads. Steel sleeves for magnet retention are normally good up to 492 MPH (220 meters/sec), while carbon fiber sleeves can handle tip speeds up to 783 MPH (350 meters/sec).

The PM rotor has a tapered Inner Diameter (ID) that allows insertion of a shaft without the use of thermal expansion/contraction. An oil fitting on the rotor face allows oil to be pumped into the space between the shaft and rotor, expanding the rotor. A matching tapered shaft is then pushed into the rotor a proscribed length (the push-in distance) using a hydraulic press. At this point the carbon fiber sleeve has the correct pre-load to retain the magnets up to the maximum specified overspeed (required for safe and reliable operation), and the shaft and rotor

combination is then inserted into the stator, maintaining the specified air gap, and is ultimately captured by the foil bearing housings.

Figure 26 is a mechanical drawing of the Beta rotor, and Figure 27 shows typical carbon fiber tubes before being cut to specified lengths.

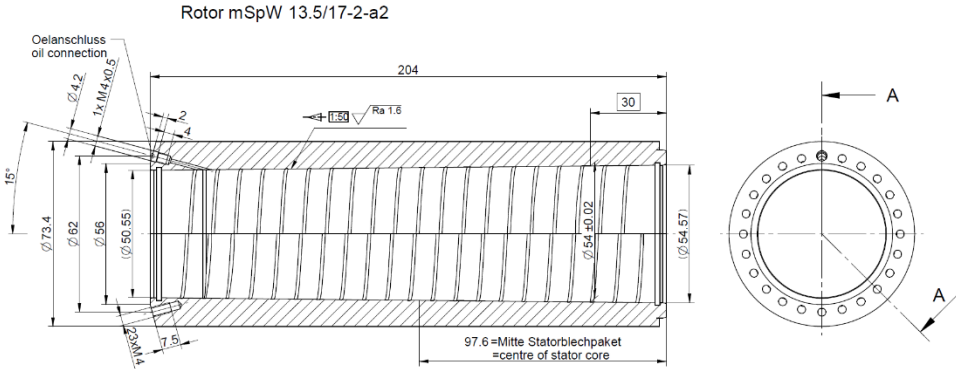


Figure 26: Mechanical Drawing of Beta PM Rotor



Figure 27: Carbon Fiber Sleeve Tubes Before Being Cut to Required Lengths

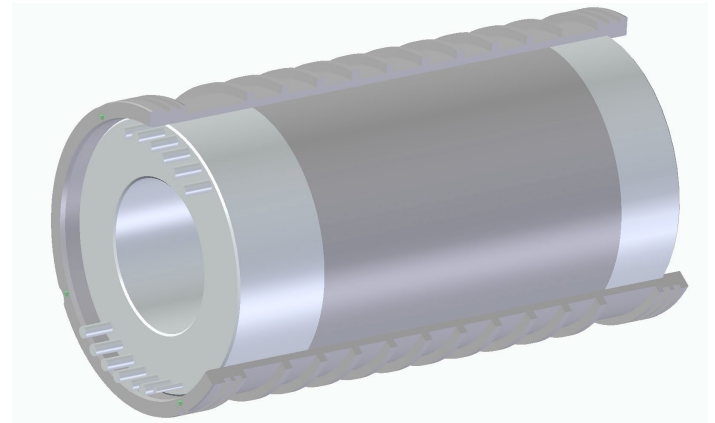
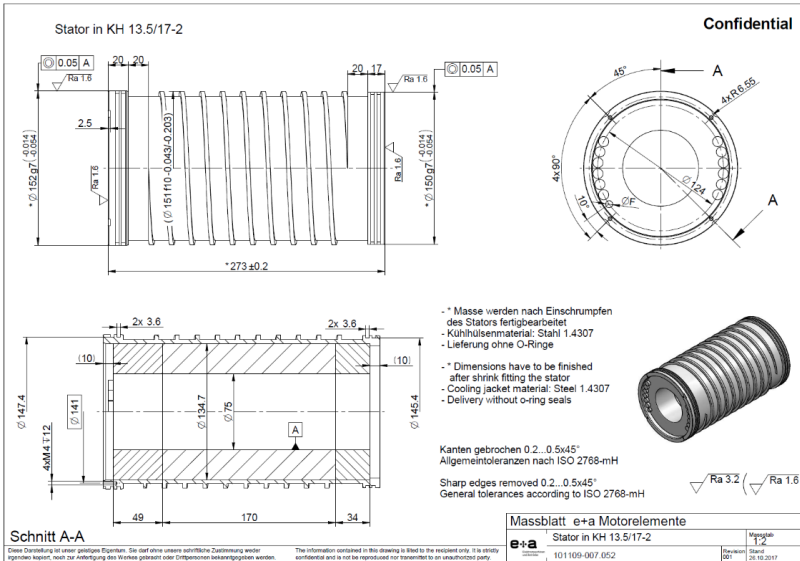


Figure 30: Mechanical Drawing of Beta Stator in Cooling Jacket (Left); 3-D Cutaway Model of Beta Stator in Cooling Jacket (Right)

Figure 28 is a Mechanical Drawing of the Beta Stator showing dimensions and placement of cable exits. During the stator design phase a number of mechanical, electrical, acoustic and electro-magnetic simulations were performed for the Alpha, Beta and Gamma stators/rotors. Figure 29 (left) presents the results of the simulation of Magnetic Flux Density in a Beta stator at rated speed and power, and Figure 29 (right) shows stators shrunk into cooling jackets, typical of the Beta Configuration; Figure 30 (left) is a Mechanical Drawing of the Beta Stator in a cooling jacket and Figure 30 (right) is a 3-D cutaway model of the Beta stator and cooling jacket.

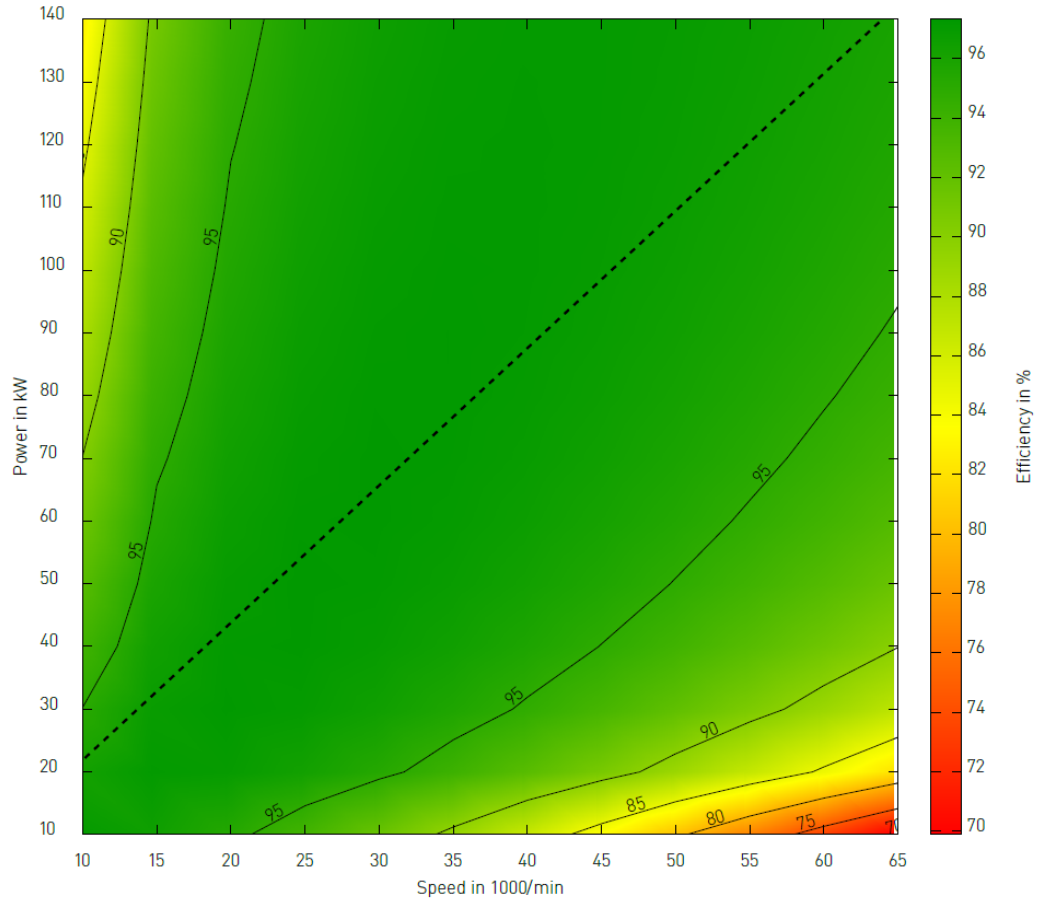
PM Stator & Cooling Jacket

The stator for the Beta machine has an OD of 5.31 inches (135mm) and a length of 9.96 inches (253mm). The end windings are encapsulated in epoxy and then covered with an Aluminum Cap (ALKA system). The ALKA cap is used for mechanical winding protection and better heat transfer from the end turns to the cooling jacket; the ALKA cap shields the magnetic field of the end turns from parts that are placed close to the end turns (like bearing housings, etc.). The stator laminations are made from high-frequency steel and the stator is shrunk into a steel cooling jacket. Three-phase cables and thermocouple wires exit the stator on one side. O-rings are fitted into slots in the cooling jacket and are used to prevent the water/glycol cooling liquid from escaping.

Generator Efficiency

The Performance Maps shown in Figure 31 (Top) and (Bottom) detail the operating efficiency of the Beta Generator over its entire performance range. For the Efficiency Map green represents high efficiency, yellow outlines areas of good efficiency, and red shows areas of poor efficiency. The data is displayed in both graph and table form. The dotted line in the Efficiency Map graph corresponds to the values given by the parameter set, i.e. the rated Power vs. Speed curve of the Beta machine. The bold numbers in the Efficiency Table correspond to values below the dotted line in the Efficiency Graph, i.e. allowed continuous operation points; the other numbers in the Efficiency Table (not Bold Face) are numbers above the dashed line in the Efficiency Graph and represent areas of overload or limited-duty operation.

PERFORMANCE MAP EFFICIENCY



PERFORMANCE MAP DATA EFFICIENCY

Efficiency in %		Speed in 1000/min											
		10.0	15.0	20.0	25.0	30.0	35.0	40.0	45.0	50.0	55.0	60.0	65.0
Power in kW	140.0	82.3	90.9	94.3	95.8	96.6	97.0	97.1	97.1	97.0	96.8	96.5	96.1
	130.0	83.4	91.5	94.6	96.0	96.7	97.1	97.2	97.1	97.0	96.7	96.4	95.9
	120.0	84.4	92.0	94.9	96.2	96.8	97.1	97.2	97.1	96.9	96.6	96.2	95.7
	110.0	85.5	92.6	95.2	96.4	97.0	97.2	97.2	97.1	96.8	96.5	96.0	95.5
	100.0	86.6	93.1	95.5	96.6	97.1	97.2	97.2	97.0	96.7	96.3	95.8	95.2
	90.0	87.7	93.6	95.8	96.8	97.2	97.3	97.2	96.9	96.5	96.1	95.5	94.8
	80.0	88.9	94.2	96.1	97.0	97.3	97.3	97.1	96.8	96.3	95.8	95.1	94.4
	70.0	90.0	94.8	96.5	97.1	97.3	97.2	97.0	96.5	96.0	95.4	94.6	93.8
	60.0	91.2	95.3	96.7	97.2	97.3	97.1	96.7	96.2	95.6	94.8	93.9	92.9
	50.0	92.5	95.9	97.0	97.3	97.2	96.9	96.4	95.7	94.9	94.0	92.9	91.8
	40.0	93.7	96.4	97.2	97.3	97.0	96.5	95.8	95.0	93.9	92.8	91.5	90.0
	30.0	95.0	96.9	97.3	97.1	96.6	95.8	94.8	93.6	92.3	90.8	89.1	87.3
	20.0	96.3	97.2	97.0	96.4	95.4	94.2	92.7	91.0	89.1	86.9	84.6	82.2
10.0	97.2	96.6	95.4	93.8	91.8	89.4	86.7	83.7	80.5	77.1	73.5	69.9	

Figure 31: Beta Generator Efficiency Map in Graph Form (Top) and Table Form (Bottom).

MULTI-LEVEL INVERTER

Conventional variable speed drives rely on motor inductance to filter the inverter's switching waveform to produce a relatively smooth motor current. The remaining switching current through the motor is referred to as "ripple current", as it appears as a triangular signal that ripples through the fundamental waveform. The simulated motor current waveform, shown in Figure 32 (left), has approximately three percent current ripple. This ripple current causes high frequency magnetic flux, which in turn, causes losses in a motor/generator by creating eddy currents in the rotor, in permanent magnets attached to the rotor, and in the stator. None of the ripple current in a Variable Speed Drive's (VFD's) waveform produces torque; it all ultimately goes to producing losses in the form of heat in the rotor and stator: see Figure 32 (right) as an example; this figure shows eddy currents induced in Permanent Magnets in a rotor by inverter harmonics (TDDi 10%, 7kHz Slip Frequency).

These losses are exponentially related to frequency, and can be very significant, even though the ripple current does not appear to be large in relation to the waveform fundamental.

To maintain acceptable rotor losses for a particular system, and especially in applications involving permanent magnet motor/generators, motor manufacturers require low ripple current, and specify a "sine filter" to be placed between the inverter and motor to provide further ripple current reduction. The cutoff frequency of this filter must be placed sufficiently above the motor's fundamental frequency to avoid excessive drive losses, but also sufficiently below the drive's switching frequency to effectively reduce the ripple current. The high motor fundamental frequency of the Beta and Gamma generators and the inclusion of a sine filter requires a much higher switching frequency than is customary for conventional variable speed drives of this power. In particular, the Gamma generator is producing 160KW while operating at a frequency of 850 Hz, and the Beta generator is producing 140KW while operating at 1,066 Hz (both are two-pole devices). The use of a sine filter between the motor/generator and a typical two-level inverter causes filter insertion loss and filter power loss, as well as the increased cost and bulk of the filter. The insertion loss reduces the voltage available to the motor/generator requiring a lower torque constant winding and therefore a higher current inverter for a given motor/generator power level. In addition to sine filter inductor losses resistors are needed to damp resonance. The power loss in these elements can be significant and the effect is to reduce two-level inverter efficiency in many systems by several percent.

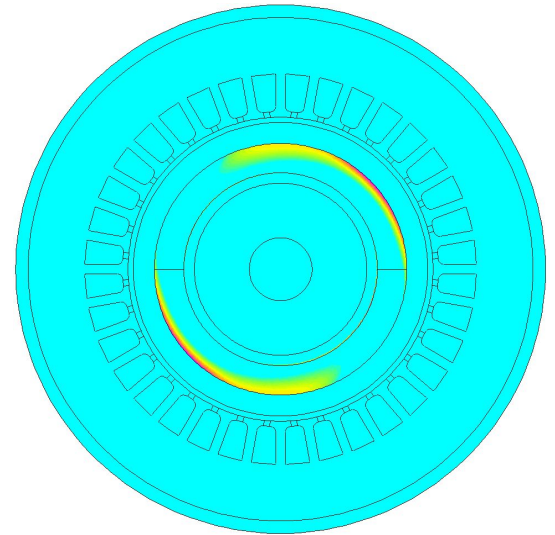
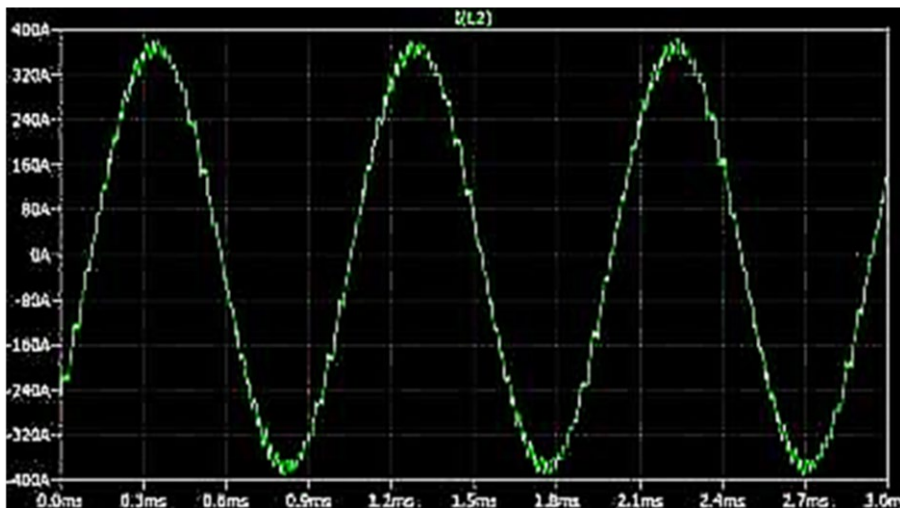


Figure 32: Ripple Current on Simulated Motor Current Waveform With Two-Level Inverter (Left); (Right) Simulation of Eddy Currents Induced on Permanent Magnets in a Rotor; Caused by Inverter Harmonics (TDDi 10%, 7kHz Slip Frequency)

Since much of the drive's loss is directly related to switching frequency, this controller employs an advanced power stage topology, called a Multi-Level Inverter (MLI), which has fewer switching losses and lower filtering requirements than conventional two-level inverters. Each time a switch changes state, there is an energy loss related to the change in voltage level. That change level for a three-level MLI is one-half the amount of that of a two-level inverter, which results in approximately 50 percent less switching loss. Additionally, the 50 percent reduction in switching voltage level also reduces the filtering requirement by 50 percent. The waveform in Figure 33 shows simulated motor phase current when driven by a three-level MLI with a sine filter. The ripple current, which is less than 0.5 percent of the fundamental, is almost undetectable by eye.

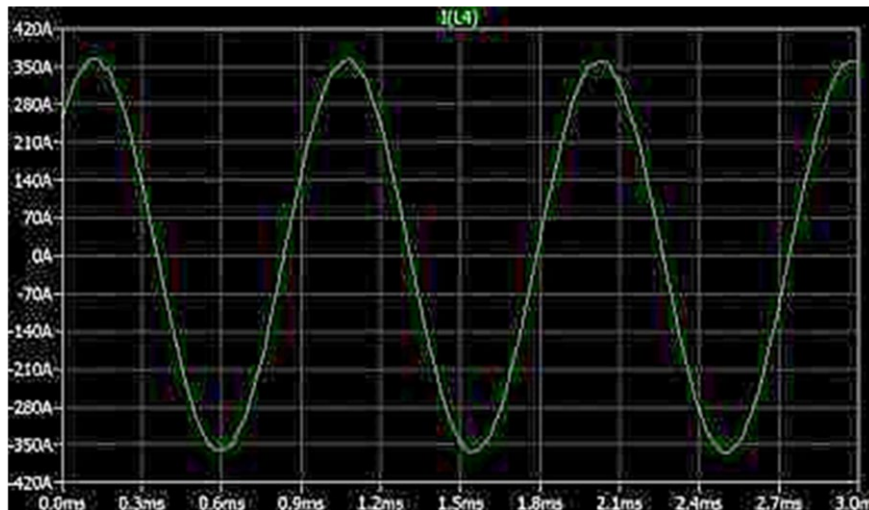


Figure 33: Ripple Current on Simulated Motor Current Waveform with Three-Level MLI & Sine Filter

The Beta/Gamma MLI operates in both motoring and generating modes. At start up, power is drawn from the utility grid and the motor accelerates the turbine to starting speed. Once up and running, the speed can be increased to the operating level, at which point the power will reverse and flow into the utility grid. Note that this behavior is automatic and happens very fast (under 50ms). Since power flow is bidirectional, a conventional diode rectifier is unsuitable for converting between the AC grid voltage and motor drive's DC link voltage.

Instead, this MLI Inverter uses an Active Front-End (AFE), which is an inverter that synchronizes to the utility grid and is controlled to produce sinusoidal currents in-phase with the sinusoidal grid voltages. The current level can be controlled by several different methods. For this system, the current is adjusted to maintain a regulated DC link voltage. AFE power flow level and direction is determined by the demand from the motor drive, which in turn, is determined by the turbine torque load at start up, and the turbine generated power when in operation.

Note that the AFE does not establish or perturb the grid frequency, but instead locks to the existing grid frequency using a Phase-Locked Loop (PLL). Similarly, the AFE does not regulate the grid voltage, but instead operates at the existing grid voltage. The variable that it does control is the 3-phase sinusoidal current, which controls the transfer of power between the generator and the grid.

The AFE is normally set to operate with near unity power factor; however, it can be commanded to have a non-unity power factor. The most straightforward way to do this is to command a reactive current level. If necessary, the software can be modified to allow a power factor command, with leading or lagging reactive current. The system would accomplish this by calculating the appropriate reactive current level based on the measured real current and commanded power factor. This method is less stable than direct setting of reactive current, particularly at light loads, and is thus less preferred.

The block diagram for the AFE/motor drive power handling path is shown in Figure 34. Recognizing that the motor has internal inductance, it becomes evident that the motor drive and AFE are functionally very similar. The key differences are in how the two systems are controlled, and how the filters and AC to DC power conversion stages are optimized. With a Multi-Level drive the capacitor/resistor networks shown in Figure 34 can be omitted, reducing complexity and power loss. The inductors between the drive and motor can also be eliminated in some cases.

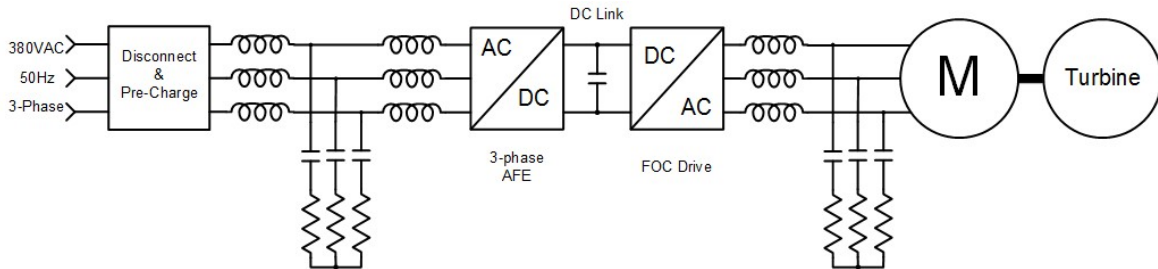


Figure 34: Motor Drive / Active Front-End Power System Block Diagram

Key system specifications for the Beta/Gamma MLI are shown in Table 2 below:

Table 2: Key Specifications for the Beta and Gamma MLI Inverter

Reliability

Operational Life	10 years
Service Interval	TBD

Electrical Specifications

General	
Power Rating	±140 kW @ 360 VAC +/-5%
Efficiency	<ul style="list-style-type: none"> < 25% load: 96% 25% to 50% load: 96% 50% load and higher: 95%
Inrush Current	None, internal soft start provided
Turbine Interface	
Motor Voltage	360 V _{RMS} at 64,000 RPM
Rated AC Output Current	270 A _{RMS}
Output Current Distortion	<3% TDD (Total Demand Distortion) at rated power
Max Electrical Frequency	1066 Hz
Max Motor Speed	64,000 RPM
Minimum Controlled Speed	<10,000 RPM
Speed Control Accuracy	±640 RPM (± 1% of Max Speed)
Speed Slew Rate	5,000 RPM/s max
Start-up Time	5s max to initialize and reach min controlled speed
Speed Settling Time	500ms max to settle within +/- 640RPM after conclusion of speed slew
Speed Under/Overshoot	±6,400 RPM max

<i>AC Grid Interface</i>	
Number of Phases	3
Nominal Grid Frequency	50 Hz / 60 Hz, Configurable
Operating Voltage	380V _{rms} , +10/-5%
Rated AC Output Current	214A _{RMS}
Phase Voltage Imbalance	3% max
Output Current Distortion	<3% TDD (Total Demand Distortion) at rated power per IEEE 519 operating conditions
<i>Circuit Isolation</i>	
Signal Terminals	3000VDC withstand voltage, 1s max Communications and I/O with respect to AC terminals
AC Terminals	3000VDC withstand voltage, 1s max AC Terminals with respect to Chassis
<i>Discrete Outputs</i>	
Voltage (max)	32 V _{DC}
Current (max)	5 mA
<i>Discrete Inputs</i>	
Voltage (min)	4.8 V _{DC}
Voltage (max)	32 V _{DC}
Current (max)	6 mA

Environmental Specifications (Indoor Use)

Operating Temperature Range	-10 to 40°C No Derating, 40 to 55°C Derating applied
Storage Temperature Range	-20 to 55°C
Operating Humidity Range	30 – 90% RH (no condensation)
Storage Humidity Range	10 - 95% RH (no condensation)
Operating Altitude	1,000 m No Derating, 1,000 to 3,000 Derated
Pollution Degree	2 (IEC 1010-1)
Ingress Protection Rating	IP52
Acoustic Noise	TBD

Mechanical Specifications

Cooling System	Liquid cooled plus internal air circulation fans
Coolant	Deionized water plus 20-25% ethylene glycol
Coolant Temperature	55°C max inlet
Coolant Flow Rate	12L/min, minimum
Weight	TBD
Dimensions (W x H x D)	1200mm x 900mm x 430mm
Vibration	MIL-810E, method 514.4 test condition I-3.3.1
Shock	Less than 20G, half sine, 11mS, unpacked
Seismic	1G seismic zone (IEEE 693 High Seismic) with seismic spectra of 0.5G

Control

The MLI motor/generator drive employs sensorless, Field Oriented Control (FOC). This scheme allows for precise control of motor torque and speed over a wide range, without use of a motor shaft position sensor. Using motor voltage and current measurements, the control software estimates rotor position by applying these real-time measurements to a model of the motor running in software. The technique used by the software is very robust, resulting in precise shaft angle tracking, and high immunity from external disturbances. The software then uses this information to optimally control the stator magnetic field in relation to the rotor angle to produce the required torque.

The motor torque command is developed by a motor speed control algorithm. The host controller sets the speed that is optimal for the intended operating power level through the specified MODBUS interface. The actual power level is determined by turbine power production. This power level can be indirectly monitored by the host controller for closed loop fuel control by reading the AFE power level (power delivered to the grid). The Human Machine Interface (HMI) is intended primarily for system monitoring, testing and setting of parameters.

Monitoring & Protection

The system includes numerous monitoring and protection functions. Where practical, warning flags are set when variables approach operational limits. Power stage temperatures and currents are examples of variables that may slowly approach limits. In such circumstances, reducing the power generated by the turbine will result in lower temperatures and currents, allowing uninterrupted operation; however, other situations could require immediate shutdown, such as loss of coolant, or a large grid voltage surge.

The system includes an emergency resistive brake to prevent turbine over-speed in the event of an unavoidable, immediate drive shutdown. The brake is capable of absorbing 140KW for up to 5 seconds (700J). Note that this brake will only operate in extreme circumstances. With normal function, the system will always attempt to shut down the turbine in a controlled manner and includes a low speed purge state for controlled cool down.

Packaging, Cooling & Interconnect

The drive is packaged in an electrical IPC52 enclosure (rated for dust and falling resistance). The complete system is shown in Figure 34 and is annotated with the names and locations of the major drive components. The enclosure size is 1200mm x 900mm x 430mm. The power stages and AFE filter damping resistors are all liquid cooled. These parts produce about 80 percent of the drive's waste heat. Liquid cooling offers several critical advantages over air cooling for this application. Most significantly, liquid cooling allows full use of power module capability. The ability for air cooled heatsinks to remove waste heat from the power modules is not enough to allow full capability operation. To maintain acceptable power device junction temperatures with air cooling, additional power modules must be connected in parallel. This would have a large impact on cost and increase unit size. In general, liquid cooling is almost always more cost effective for high speed drives of this class. The maximum heat removed by the coolant will be approximately 6000W with the Beta 140KW generator. The filter inductors, DC link chopper resistor and emergency brake resistors use forced air cooling.

All power connections are hard-wired to screw-type or compression terminals. Control cables interface through appropriately sized connectors. Special attention was given to cabling between the drive and the motor. The high frequency motor current will limit the maximum practical wire diameter due to the skin effect and wire sizes above about 5mm diameter exhibit higher AC resistance than DC resistance. The drive is located as close as practical to the motor.

Figure 35 shows the actual Beta/Gamma MLI in its enclosure; the figure is annotated to identify the various elements of the system.



Figure 35: Complete Beta/Gamma MLI Controller in IPC52 Cabinet

Figure 36 shows the Block Diagram for the MLI, primarily outlining the System controller and its connections to the Pre-Charge system, the AFE, the braking circuit, the Utility Grid and the Turbine.

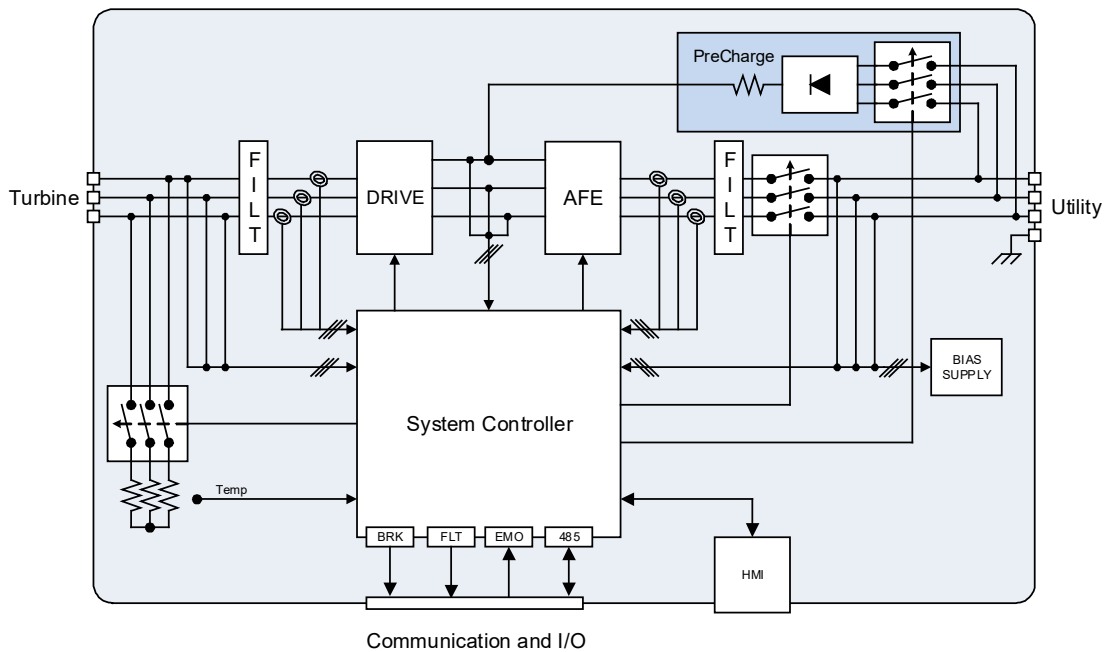


Figure 36: Beta/Gamma MLI Controller Block Diagram

The Beta/Gamma MLI Controller also has the following functionality:

Ride-Thru Supply - Provides bias power from the DC link when the AC input falls below 50 percent of nominal, and the AC input bias supply can no longer support the load. This is necessary to support uninterrupted operation with a short-term reduction in AC grid voltage.

DC Chopper Resistor - Absorbs excess power when the load decreases quickly, compensating for the turbine's low power slew rate. It is periodically activated in normal operation. It is switched with an IGBT using PWM and is controlled to absorb no more power than necessary. The DC Chopper Resistor in the Beta/Gamma MLI is designed to absorb 500 KJ while the turbine power is decreased to support a lower power requirement.

Anti-Islanding - While online the MLI provides anti-islanding protection by monitoring the grid voltage and frequency for instability. Islanding can occur when a distributed generation source continues to energize a portion of the utility grid (the island) after the utility has stopped providing power. The MLI Controller treats the island condition like a fault, shutting off both the drive and AFE and closing the brake contactor. Anti-Islanding can be enabled or disabled by the user.

CONCLUSIONS

An advanced energy generation system using a Gas Turbine Engine and a direct drive PM generator, both with foil bearings, and a Multi-Level PWM Inverter were designed, built and successfully tested. Goals of a smaller footprint, elimination of oil as a lubricant, higher performance and lower cost were achieved by eliminating the original gearbox, its oil system and the large low speed motor & controller; matching the speed of the GTE and the PM Generator by using a high-speed, flexible coupling and employing a high-frequency MLI Inverter simplified the system architecture, increased system reliability and efficiency, and significantly decreased the overall size of the resulting package.

REFERENCES

1. Rotordynamics Analysis of 140kW Micro Gas Turbine Rotor, November 12, 2017, Dr. Daejong Kim, Bellkim Energy LLC